J. For. Res. (2021) 32:713–723
https://doi.org/10.1007/s11676-020-01148-0

ORIGINAL PAPER

Nitrogen availability regulates deep soil priming effect by changing microbial metabolic efficiency in a subtropical forest

Chang Liao[1,2] · Qiuxiang Tian[1] · Feng Liu[1]

Received: 18 January 2020 / Accepted: 18 February 2020 / Published online: 19 May 2020

Abstract In terrestrial ecosystems, deep soils (below 30 cm) are major organic carbon (C) pools. The labile carbon input could alter soil organic carbon (SOC) mineralization, resulting in priming effect (PE), which could be modified by nitrogen (N) availability, however, the underlying mechanism is unclear for deep soils, which complicates the prediction of deep soil C cycling in response to N deposition. A series of N applications with ^{13}C labeled glucose was set to investigate the effect of labile C and N on deep SOC mineralization. Microbial biomass, functional community, metabolic efficiency and enzyme activities were examined for their effects on SOC mineralization and PE. During incubation, glucose addition promoted SOC mineralization, resulting in positive PE. The magnitude of PE decreased significantly with increasing N. The N-regulated PE was not dependent on extracellular enzyme activities but was positively correlated with carbon use efficiency and negatively with metabolic quotient. Higher N levels resulted in higher microbial biomass and SOC-derived microbial biomass than lower N levels. These results suggest that the decline in the PE under high N availability was mainly controlled by higher microbial metabolic efficiency which allocated more C for growth. Structural equation modelling also revealed that microbial metabolic efficiency rather than enzyme activities was the main factor regulating the PE. The negative effect of additional N suggests that future N deposition could promote soil C sequestration.

Keywords Deep soil · Priming effect · Community-level physiological profiling · Soil enzyme activity · Microbial metabolic efficiency

Introduction

Deep soil below 30 cm contributes about half of the total carbon (C) stock in soil profiles (Rumpel and Kögel-Knabner 2011). Small changes in deep soil C cycling have significant effects on global C budgets. Labile C input could accelerate or inhibit the mineralization of SOC, causing priming effect (PE) (Kuzyakov et al. 2000). Previous studies have confirmed the positive PE, an increase in decomposition rates of SOC in deep soil, and its magnitude was widely found to be larger than that in topsoil (Wang et al. 2014a; Zhang et al. 2015; Tian et al. 2016).

Nitrogen (N) is an important biological element and its availability can mediate the magnitude and direction of the PE (Fierer et al. 2003; Fang et al. 2018; Hicks et al. 2019). However, the effects of N availability on SOC mineralization have been controversial, with reports of positive (de Graaff et al. 2006), negative (Janssens et al. 2010; Blagodatskaya et al. 2007) or no effects (Liljeroth et al. 1994). Multiple

Project funding: This research was supported by the Natural Science Foundation of China (Grant numbers 31870465, 31600377, 31700462).

The online version is available at http://www.springerlink.com

Corresponding editor: Yu Lei.

Electronic supplementary material The online version of this article (https://doi.org/10.1007/s11676-020-01148-0) contains supplementary material, which is available to authorized users.

✉ Feng Liu
liufeng@wbgcas.cn

[1] CAS Key Laboratory of Aquatic Botany and Watershed Ecology, Wuhan Botanical Garden, Chinese Academy of Sciences, Wuhan 430074, People's Republic of China

[2] University of the Chinese Academy of Sciences, Beijing 100049, People's Republic of China

divergent hypotheses (such as stoichiometric decomposition and microbial N mining limitation) have been proposed to explain these varied phenomena (Melillo et al. 1982; Hessen et al. 2004; Fang et al. 2018; Liu et al. 2020). Enhanced PE with the addition of N was explained by the "stoichiometric decomposition" theory, which assumes that microbial activity and SOC mineralization rates are both highest when C and N inputs correspond to the cellular and physiological demands of the soil microorganisms (Melillo et al. 1982; Hessen et al. 2004). In this case, PE is assumed to be greater in soils with high N availability, i.e., low C: N. The coupled PE and the shift of microbial activities, including enzyme activities, support this theory (Fang et al. 2018). In contrast, the declined PE with the addition of N usually has been explained by the "microbial N mining" theory which assumes that an increase in N availability will shift the microbial utilization of N source toward the added N, hence reducing the microbial activity in mining SOC (N-containing substrates in soil), and consequently reduce the magnitude of PE (Moorhead and Sinsabaugh 2006; Craine et al. 2007). Changed microbial functional activities and the decrease of N-acquiring enzyme activities can verify this theory (Chen et al. 2014).

Recently, the declined PE under high N availability was found to be controlled by high microbial metabolic efficiency, but not microbial activity (Chen et al. 2018). Increased N availability may enhance microbial metabolic efficiency for energy needs and N to balance anabolic and catabolic reactions, and then decrease SOC mineralization and the magnitude of PE. Deep soil can acquire labile C and N from root systems and flow paths. How extra N input might regulate deep soil C mineralization and its potential mechanism are unknown. These knowledge gaps would constrain the prediction of deep soil C response to future global changes.

In order to explore the effects of N availability on the PE in forest deep soils, an incubation experiment was designed with different C: N levels. Soil microbial biomass C (MBC), microbial functional diversity, enzyme activities, and microbial metabolic efficiency were assessed after 7 days on their relationships with SOC mineralization and the PE. In this study, we hypothesized that: (1) higher N availability could significantly reduce the PE; and, (2) N availability mediated the PE mainly by altering microbial metabolic efficiency.

Materials and methods

Soil collection

Soil samples were collected from the 30–60 cm layer in an evergreen-deciduous broad-leaved mixed forest located in the Badagongshan National Research Reserve, Hunan Province (29° 46.04′ N, 110° 5.24′ E) in the mid-subtropical zone. The forest is dominated by species of *Fagus lucida* Rehder & E.H. Wilson, *Cyclobalanopsis multinervis* W. C. Cheng & T. Hong, *Cyclobalanopsis gracilis* (Rehder & E. H. Wilson) W. C. Cheng & T. Hong, *Carpinus viminea* Lindley, *Schima parviflora* Cheng et Chang ex Chang, *Sassafras tzumu* (Hemsl.) Hemsl, and *Castanea seguinii* Dode. (Wang et al. 2014b). The climate is a subtropical mountain humid monsoon with annual average precipitation of 2105 mm. Temperatures range from 0.1 °C in January to 22.8 °C in July, with an annual mean of 11.5 °C. The soil is classified as a well-drained, fine-textured Hapludalf (US Soil Taxonomy Series).

The samples were homogenized, taken to the laboratory and passed through a 2- mm sieve. Roots and visible residues were removed manually and samples were stored in at < 4 °C until incubation. Total C and N contents were 35.7 mg g^{-1} and 2.67, respectively. Soil pH was 5.0. The $\delta^{13}C$ was − 25.6‰.

Experimental design and soil incubation

The incubation experiment included six treatments with six replicates: soil with no addition (Control), soil with glucose addition (C-only), soil with glucose and four N levels with C: N ratios of 40, 20, 10 and 2.5 (Table 1). The added glucose-C corresponded to 100% of soil microbial biomass C (MBC) based on results from soils after 5 days of pre-incubation. Fresh soil samples, 20 g dry weight, were incubated into a 250 mL triangular flask following adjustment of moisture to 65% water-holding capacity by adding deionized H_2O. All samples were pre-incubated at 20 °C for 5 days. After pre-incubation, 3 mL of the appropriate glucose solution (uniformly labeled, $\delta^{13}C = 2000‰$) with or without an N source (NH_4NO_3) was added to each sample. For the control, 3 mL of deionized H_2O was added.

Table 1 Total labile C and N addition to the soil in the six treatments

Treatment	Applied C (mg C g^{-1} dry soil)	Applied N (μg g^{-1}dry soil)
Control	0	0
C-only	160	0
C:N = 40	160	4
C:N = 20	160	8
C:N = 10	160	16
C:N = 2.5	160	64

Measurement of CO_2 fluxes

Soil respiration was measured on days 0, 1, 4, 7, 13 and 20. At each time, a 10 mL sample of headspace was extracted from the flask and injected into an infrared gas analyzer (IRGA; EGM-4, PP Systems, Amesbury, MA, USA) to determine initial CO_2 concentration. The replicates were then returned to the 20 °C incubator for several hours. A 10 mL sample of headspace was again extracted from each flask to determine the final CO_2 concentration in order to calculate the respiration flux rate. When measuring ^{13}C of CO_2, another three replicates of each treatment were flushed with CO_2-free air for 5–10 min (air through a soda-lime column) to remove CO_2 in the flasks. The ports were then closed and flasks returned to the 20 °C incubator for several hours according to the CO_2 release rate to ensure CO_2 concentration reaches at least 400 μmol mol^{-1}. Gas samples were collected in an evacuated gas vial to determine the $\delta^{13}C$ of CO_2 (Carbon Isotope Analyzer 912-0003, LGR, USA) to calculate proportionate contributions of respiration sources. At the end of 7 days of incubation, destructive samplings with three replicates were performed to determine the MBC, community-level physiological profiles, and soil enzyme activities.

Microbial biomass as well as the isotope signature analysis in MBC

Soil samples were divided into two 10-g fresh samples; one was fumigated with ethanol-free chloroform for 24 h followed by extraction with 0.05 mol L^{-1} K_2SO_4 after shaking for 30 min and the other was extracted immediately with 0.05 mol L^{-1} K_2SO_4, also shaking for 30 min. The extraction was then determined by TOC (Vario TOC Elemental, Germany).

The $\delta^{13}C$ of the K_2SO_4 extract solution was determined by sodium persulfate oxidation to transform the liquid into gas as modified by Midwood et al. (2006) and Garcia-Pausas and Paterson (2011). A 10- mL water solution (fumigated and unfumigated) was added to a 250 mL reaction bottle and 100 μL of 1.3 mol L^{-1} phosphoric acid solution was then added to remove inorganic C. A 200 μL of 1.05 mol L^{-1} sodium persulfate was then added. For the blank control, 10 mL ultrapure water was added, and the other steps were the same. The reaction bottle was capped, flushed with CO_2-free air, heated in a 90 °C water bath for 30 min to promote oxidation. The gas in the bottle was transferred into an airbag to determine the CO_2 isotope value by the Carbon Isotope Analyzer 912–0003.

Measurement of soil enzyme activity

The activities of five enzymes, β-glucosidase (BG), N-acetylglucosaminidase (NAG), xylanase (XYL), cellobiohydrolase (CBH), and leucine aminopeptidase (LAP) were measured using 96-well microtiter plates (Table S1). Eight replicate wells per sample per assay were treated following a modified method from Saiya-Cork et al. (2002). 1 g sample of fresh soil was suspended in 100 mL of a 50 mmol sodium acetate buffer (pH = 5), homogenized and stirred with a magnetic stirrer. The activities of BG, NAG, CBH, XYL and LAP were analyzed fluorometrically by adding 50 μL 4-methylumbelliferyl-β-D-glucopyranoside (200 μmol L^{-1}), 4-methylumbelliferyl-N-acetyl-β-D-glucosaminide dehydrate (200 μmol L^{-1}), 4-methylumbelliferyl-β-D-cellobioside (200 μmol L^{-1}), 4-methylumbelliferyl-β-D-xylopyranoside (200 μmol L^{-1}) and L-leucine-7-amino-4-methylcoumarin (200 μmol L^{-1}) plus 200 μL of soil suspension, respectively. Blank wells were added 50 μL of acetate buffer plus 200 μL of soil suspension; negative control wells were added 50 μL of substrate solutions plus 200 μL of acetate buffer. The quench standard wells were added 50 μL of standard solution (10 μmol L^{-1} 4-methylumbelliferone for BG, NAG, CBH and XYL or 7-amino-4- methylcoumarin for LAP) plus 200 μL of soil suspension. The black microplates were incubated in the dark at 20 °C for 4 h. Fluorescence was measured using the microplate reader (M200 PRO, Tecan, Austria) with excitation at 365 nm and emission at 450 nm.

Community-level physiological profiles (CLPPs) of microbial communities

BIOLOG Eco-Plates TM system (Biolog, Hayward, CA, USA) containing 31 carbon sources were used to measure the CLPPs of microbial communities to represent the microbial functional community. The Biolog technique is widely used to evaluate the functional diversity of soil microbial communities and is based on the principle that the color developments of tetrazolium dye reduction after the substrate utilization]. 5 g sample of fresh soil was added to a 50 mL 0.85% sterilized NaCl solution and shaken for 30 min. 1 mL suspension was taken out into a 1.5 mL centrifuge tube immediately. The soil solution was centrifuged at 10,000 rpm for 20 min, then discarded the supernatant. 1 mL 0.85% sterilized NaCl solution was added into the centrifuge tube, the solution mixed well by shaking on a vortex oscillator for 5 min, and then centrifuged at 10,000 rpm for 20 min. The process was repeated twice to remove the carbon source and then the supernatant was discarded. 1 mL 0.85% sterilized NaCl solution was added again, shaken on the vortex oscillator for 5 min and centrifuged at 2000 rpm for 1 min. 1 mL supernatant

was taken out and diluted 10 times with 0.85% sterile NaCl solution. The diluent was inoculated into each well of the ECO plate with 150 µL, and the inoculated ECO-plates was incubated at 20 °C. Absorbance was measured at 590 nm and 750 nm with a microplate reader (Multilabel Plate Readers, M200 PRO, Tecan, Austria) at 12 h intervals for 136 h.

Calculations

Soil CO_2 efflux rates derived from native SOC during the incubation were calculated as:

$$C_{treat(soc)} = C_{treat} \times \left(\frac{\delta^{13}C_{treat} - \delta^{13}C_{glucose}}{\delta^{13}C_{control} - \delta^{13}C_{glucose}} \right) \quad (1)$$

where $C_{treat(SOC)}$ and C_{treat} are the soil CO_2 efflux rate derived from SOC (µg CO_2-C g^{-1} soil C h^{-1}) and total soil CO_2 efflux rate (µg CO_2-C g^{-1} soil C h^{-1}) in treatments with glucose, $\delta^{13}C_{treat}$ and $\delta^{13}C_{control}$ are the isotopic signature of the released CO_2 in treatments with glucose and control without glucose, δ^{13} $C_{glucose}$ is the isotopic signature of the glucose C added to the samples. An underlying assumption of this equation is that the isotopic signatures of the glucose and SOC are homogeneous.

During incubation, the priming effect induced by glucose was calculated by comparing the SOC mineralization in glucose- amended samples with control samples:

$$PE(\%) = \frac{C_{treat(soc)} - C_{control}}{C_{control}} \times 100 \quad (2)$$

where $C_{control}$ is CO_2 emission in control without glucose addition.

The SOC-derived MBC was calculated according to a simple isotopic mixing model:

$$MBC_{treat(soc)} = MBC_{treat} \times \left(\frac{\delta^{13}C_{glucose} - \delta^{13}MBC_{treat}}{\delta^{13}C_{glucose} - \delta^{13}MBC_{control}} \right) \quad (3)$$

where $MBC_{treat(SOC)}$ and MBC_{treat} are the microbial biomass C derived from SOC (µg g^{-1}) and total microbial biomass C (µg g^{-1}) in treatments with glucose, the δ^{13}MBC_{treat} and δ^{13}MB$C_{control}$ are the $\delta^{13}C$ value of MBC in the treatments with glucose and the control, respectively.

The two common parameters of microbial metabolic efficiency, carbon use efficiency (CUE), and metabolic quotient (qCO_2) were calculated. CUE was estimated based on C: N stoichiometry (Sinsabaugh et al. 2016) following Eqs. (4) and (5):

$$CUE_{C:N} = CUE_{max} \times \frac{S_{C:N}}{S_{C:N} + K_N} \quad (4)$$

$$S_{C:N} = \frac{1}{EEA_{C:N}} \times \frac{B_{C:N}}{L_{C:N}} \quad (5)$$

where $S_{C:N}$ is an index that represents the degree of the allocation of exoenzyme activity offsets, the imbalance between the C and N composition of labile resources, and the composition of microbial biomass. On the basis, The K_N, the half-saturation constant was assumed to 0.5. The CUE_{max} was the maximum value of microbial growth efficiency based on thermodynamic constraints and was assumed to 0.6. $EEA_{C:N}$ is the ratio of exoenzyme activities that acquired C and N sources directly from the soils and is calculated as BG/(NAG + LAP). $B_{C:N}$ is the molar ratios of MBC and MBN and the $L_{C:N}$ is the ratio of labile C and N. The qCO_2 was estimated as the total soil CO_2 efflux rate per unit of MBC.

Statistical analyses

Data are the means of three replicates with standard errors (SE). Duncan test was used to identify statistical differences among each treatment at $p < 0.05$. Repeated ANOVA was used to determine the significant difference in PE and cumulative primed C along the incubation time. The effects of N availability on soil enzyme activities, MBC as well as PE were analyzed by a one-way ANOVA analysis of variance. The color development readings of the wells at 136 h were chosen to reveal the overall microbial utilization of each substrate. The 31 C sources were divided into six groups by their chemical structures: amines, amino acids, carbohydrates, carboxylic acids, polymers and miscellaneous (Derrien et al. 2014). Principal component analysis (PCA) analyzed the effect of N availability on the relative substrate utilization patterns of soil microbial communities. Correlation analysis quantified the relationships between PE and enzyme activities, qCO_2, and CUE to reveal the underlying mechanisms in mediating PE. Mantel test at 999 permutations was used to determine the impact of the microbial functional community (the relative substrate utilization of carbohydrates, carboxylic acids, amino acids, polymers, amines and miscellaneous) on PE based on Euclidean distance. ANOVA and correlation analyses were performed using SPSS version 21.0 for Windows. The PCA and Mantel tests used the "vegan" package in R version 3.5.1.

Structure equation modelling was further used to assess the direct and indirect effects of N availability on enzyme activities, microbial functional communities, microbial metabolic efficiency and PE. The fitness of the final model was evaluated using the goodness of fit. The structural equation

modelling analyses were conducted using the "plspm" package in R version 3.5.1.

Results

Effect of glucose and N addition on PE

Glucose addition increased SOC mineralization, leading to a positive PE (Fig. 1a, b). The magnitude of PE was significantly affected by the level of N addition and by the incubation time. The PE peaked once glucose was added and then decreased gradually with time. The magnitude of PE decreased significantly with increasing levels of N except at day 20 where the PE was similar among treatments. The cumulative primed C during the first 7 days accounted for 64–82% of the primed C during the 20-day incubation (Fig. 1b).

Effects of glucose and N addition on soil microbial processes

Glucose and the addition of N significantly increased MBC and the SOC-derived MBC. With increasing levels of N, total MBC and SOC-derived MBC increased significantly (Fig. 2a, b).

C-only addition increased soil microbial qCO_2 but had no effect on CUE. When N was added in combination with glucose, microbial qCO_2 decreased. Conversely, the CUE increased with the level of N addition (Fig. 2c, d). C-only addition had no significant effect on soil enzyme activities. When N was added with glucose, the activities of the enzymes BG, CBH, NAG, LAP and XYL increased gradually with increasing N (Fig. 3).

PCA analysis revealed that the pattern of substrate utilization by soil microorganisms was affected by the addition of glucose and N. Glucose and N addition increased the relative utilization of carbohydrates, carboxylic acids and amines. The microbial community under lower N levels (C-only and C: N ratio = 40) had greater relative utilization of carbohydrates, carboxylic acids and amino acids than under higher N levels. Higher N availability might improve the relative utilization of polymers (Fig. 4).

Effect of enzyme activities, CUE, qCO_2, the microbial functional community on PE

There were significantly negative relationships between PE and enzyme activities (Table S2). The PE was negatively correlated with CUE and positively with qCO_2 (Fig. 5a, b). Mantel tests showed that the PE was closely related to the microbial functional community ($R = 0.35$, $p < 0.01$).

Indirect and direct effects of N addition on PE

Structural equation modelling analysis was carried out to evaluate the mechanisms of the effects of N availability on PE and the main factors regulating PE. The modelling explained 83% of the variation in the PE (Fig. 6). Among the factors, only microbial metabolic efficiency showed the highest and most significant direct effects on PE. The soil microbial functional community slightly affected the PE through its indirect effect on microbial metabolic efficiency. N availability directly affected extracellular enzyme activities, the microbial functional community and its metabolic efficiency significantly. N availability significantly affected the PE through its indirect effect on microbial metabolic efficiency and the microbial functional community. Extracellular enzyme activities had minor effects on the PE and microbial metabolic efficiency.

Discussion

Glucose addition increased SOC mineralization in deep soil, resulting in positive PE. This result is consistent with Wang et al. (2014a) and Naisse et al. (2015). The positive PE may be a result of microbial "co-metabolism" where microorganisms utilize labile C as a source of energy to degrade SOC (Blagodatskaya and Kuzyakov 2008). Their theory

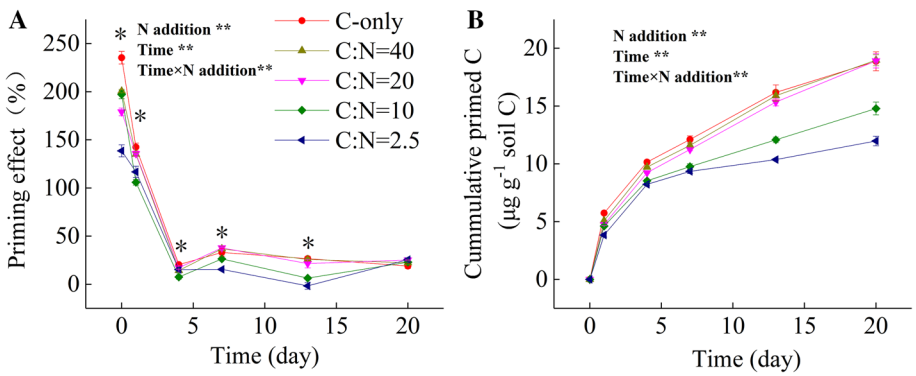

Fig. 1 Effects of glucose and N addition on **a** priming effect and **b** cumulative primed C during 20 days incubation. Results are means ± SE (n = 3). ** $p < 0.01$; * $p < 0.05$

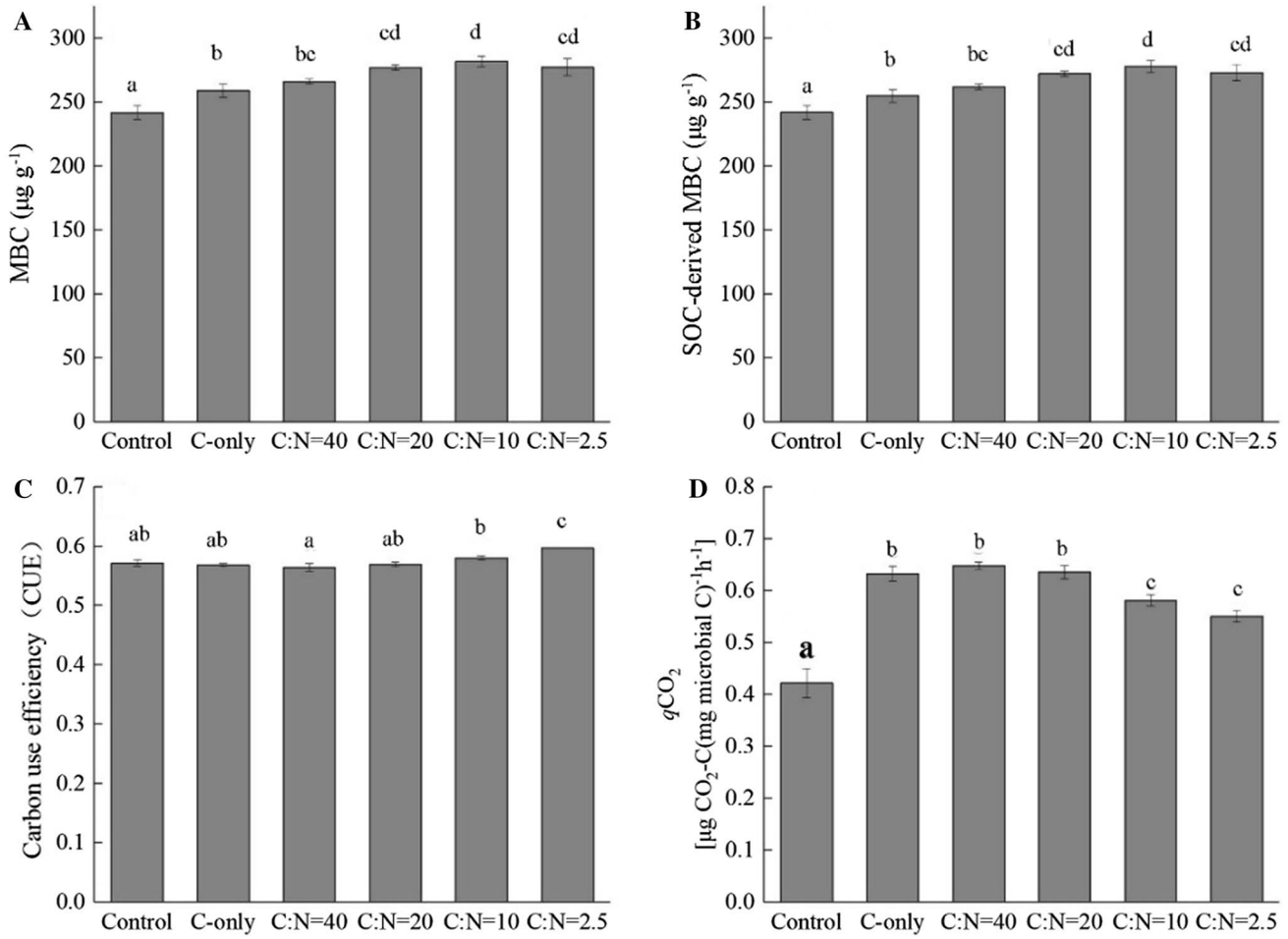

Fig. 2 Effects of glucose and N addition on **a** total MBC, **b** SOC-derived MBC, **c** carbon use efficiency and **d** *q*CO2 after 7 days incubation. Significant differences between treatments are marked by lowercase letters. Results are means ± SE (n = 3)

is supported in this study by the increased total MBC and SOC-derived MBC after glucose addition (Fig. 2a, b). Similar to previous reports (Chen et al. 2014; Zhang et al. 2019), PE was detected immediately following the addition of labile C and most occurred in the early stage of incubation. Once the external substrates exhausted, the magnitude of PE decreased. The increase of MBC after labile C addition suggests that microorganisms utilize the labile C as an energy source to synthesize biomass (Morrissey et al. 2017). The results indicate that the labile C substituted for a part of the microbial constituents, which was regarded as apparent PE. This was mainly due to the accelerated microbial turnover or pool substitution (Blagodatskaya and Kuzyakov 2008; Blagodatsky et al. 2010). However, we observed the increased SOC-derived MBC with the addition of N, suggesting that the apparent PE was not the main source of PE in our study.

As expected, the addition of N decreased the magnitude of the PE, confirming previous findings (Wang et al. 2014a; Fang et al. 2018). A common explanation for the negative effect of N availability on PE is the "microbial N mining" theory which considers that microorganisms degrade SOC to gain N (Craine et al. 2007). Accordingly, an increase in N availability will reduce microbial activity in mining SOC (N-containing substrates in the soil) and consequently reduce the magnitude of PE (Chen et al. 2014). However, enzyme activities did not decrease at higher N levels (Fig. 3), and the relative utilization of N-containing substrates by microorganisms was similar among treatments. These results suggested that the "microbial N mining" theory and the variation of microbial activities do not explain lower PE with the addition of N. Other mechanisms appear to be responsible for this phenomenon.

Interestingly, the PE was positively correlated with qCO_2 and negatively correlated with CUE. The CUE and qCO_2 were two common parameters of microbial metabolic efficiency (Pinzari et al. 2017; Chen et al. 2018). Higher CUE and lower qCO_2 values suggest that microbes allocate more C and energy for their growth rather than for respiration, then reducing CO_2 efflux and PE. However, the CUE was difficult to measure directly. It could be estimated indirectly

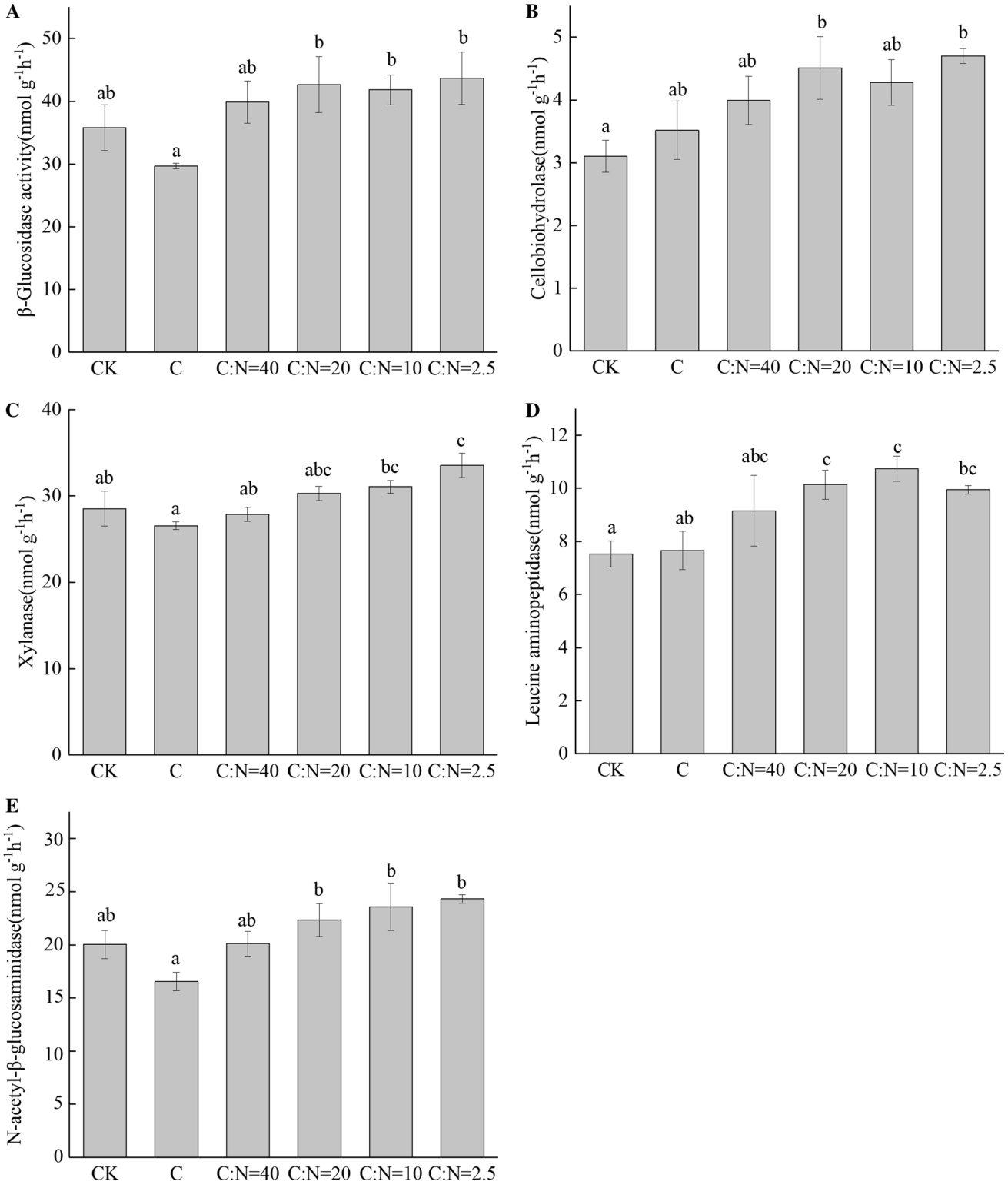

Fig. 3 Effect of glucose and N addition on extracellular enzyme activities: **a** β-glucosidase (BG), **b** cellobiohydrolase (CBH), **c** xylanase (XYL), **d** leucine aminopeptidase (LAP), **e** N-acetylglucosaminidase (NAG) after 7 days incubation. Significant differences between treatments are marked by lowercase letters. Results are means ± SE (n = 3)

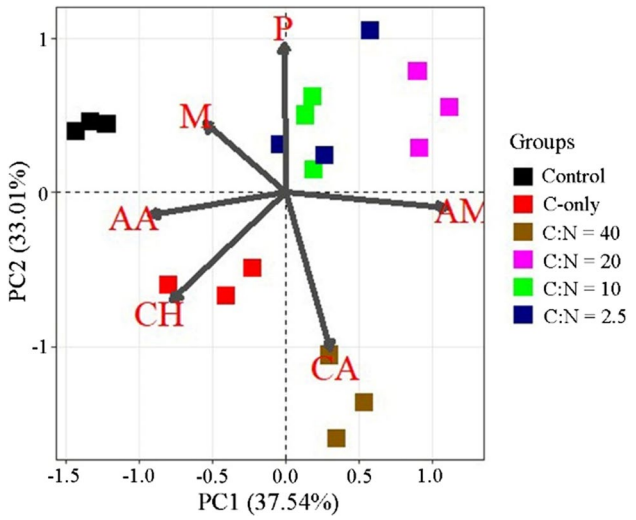

Fig. 4 Principal Component Analysis (PCA) of microbial substrate utilization pattern for glucose and N addition after 7 days incubation. Thirty-one substrates were separated into six groups: *CH* carbohydrates, *CA* carboxylic acids, *AA* amino acids, *P* polymers, *AM* amines, *M* miscellaneous

according to C and N stoichiometry of the SOC and the microbial biomass C and N, as well as the stoichiometry of extracellular enzymes (Sinsabaugh et al. 2016). Therefore, we used the methods to estimate the microbial CUE on the 7th day under different N availabilities.

In this study, higher levels of N resulted in significantly higher CUE and lower qCO_2 (Fig. 2c, d), suggesting that the addition of N regulated the PE by changing microbial metabolic efficiencies. Recent research has demonstrated that N availability regulates microbial metabolic efficiency and then soil C cycling (Chen et al. 2018; Liu et al. 2018). Under N-deficient conditions, i.e., a high C: N disparity between the substrate and microbial biomass, microorganisms may reduce their CUE to maintain a balanced biomass C:N (Manzoni et al. 2012; Mooshammer et al. 2014; Sinsabaugh et al. 2016). Conversely, CUE will increase under conditions of high N availability. The increase in MBC and SOC-derived MBC at higher N levels confirms that more C was allocated for microbial growth. Additionally, our results show that higher N availability promoted microbial relative utilization of complex C substrates towards polymers and suppressed the microbial relative utilization of simple C substrates towards carbohydrates and carboxylic acids (Fig. 6). Previous studies also demonstrate that the addition of N improves the microbial ability to breakdown complex C forms (Currey et al. 2010; Jiang et al. 2016). Since the use efficiencies of complex substrates were higher than simple substrates ((Bölscher et al. 2016), the variation in microbial functional communities also possibly accounted for the variation in microbial metabolic efficiency with the addition of N.

Structural equation modelling further demonstrated that microbial metabolic efficiency was the main factor that regulated the PE, and enzyme activities had no effect. The direct effect of the microbial functional community on its metabolic efficiency indicates that the microbial functional community could indirectly affect the PE by altering its metabolic efficiency.

Conclusions

The results indicate that labile C input serves as an energy source to stimulate microbial growth and activities, which

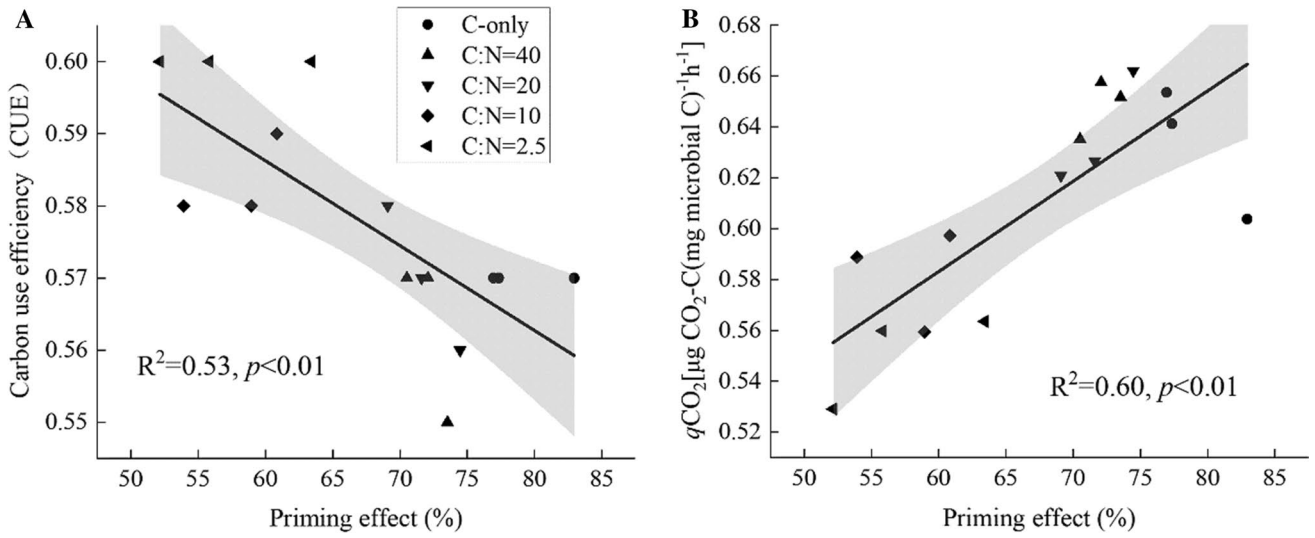

Fig. 5 Relationship between **a** priming effect and carbon use efficiency and **b** qCO_2 after 7 days incubation

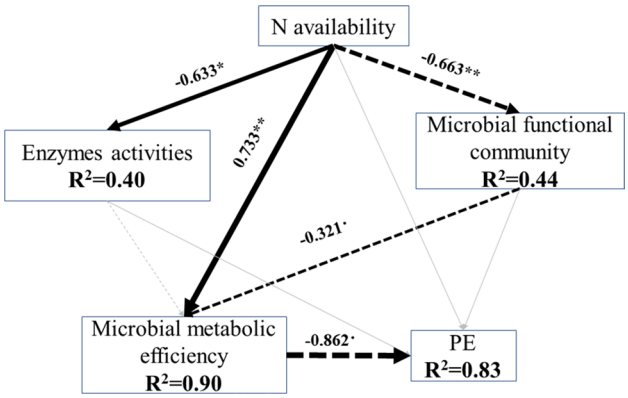

Fig. 6 Structural equation modeling assessing direct and indirect effects of N availability on PE. Numbers adjacent to arrows indicate the effect size of the path coefficient; arrow width is proportional to the magnitude of the relationship. Black solid and dashed arrows indicate positive and negative relationships, respectively. Grey arrows indicate insignificant relationships. Significance levels are:$^{**}p<0.01$; $^{*}p<0.05$; $\cdot p<0.07$. The goodness of fit was 0.61

resulted in a positive priming effect. The increased microbial biomass carbon (MBC) and the soil organic carbon-derived MBC suggest that the positive priming effect was caused by "co-metabolism". Higher nitrogen availability suppressed the priming effect, which was positively correlated with the metabolic quotient (qCO_2) and negatively with the carbon use efficiency, suggesting that the decreased priming effect with higher nitrogen levels was due to increased microbial metabolic efficiency (Fig. 7). Higher nitrogen availability shifted the microbial relative substrate utilization towards polymers. Hence, higher nitrogen availability combined with changes in microbial functional community structure led to higher microbial metabolic efficiency and consequently lower priming effect (Figs. 6, 7). These results emphasize the importance of microbial metabolic efficiency in regulating carbon dynamics and to better understanding subsoil carbon dynamics in the context of future nitrogen deposition intensification. The addition of nitrogen favors subsoil carbon sequestration by reducing the priming effect. However, further research is needed for other forest ecosystems since this study focused only on a subtropical mixed forest.

Compliance with ethical standards

Conflict of interest The authors declare that they have no conflict of interest.

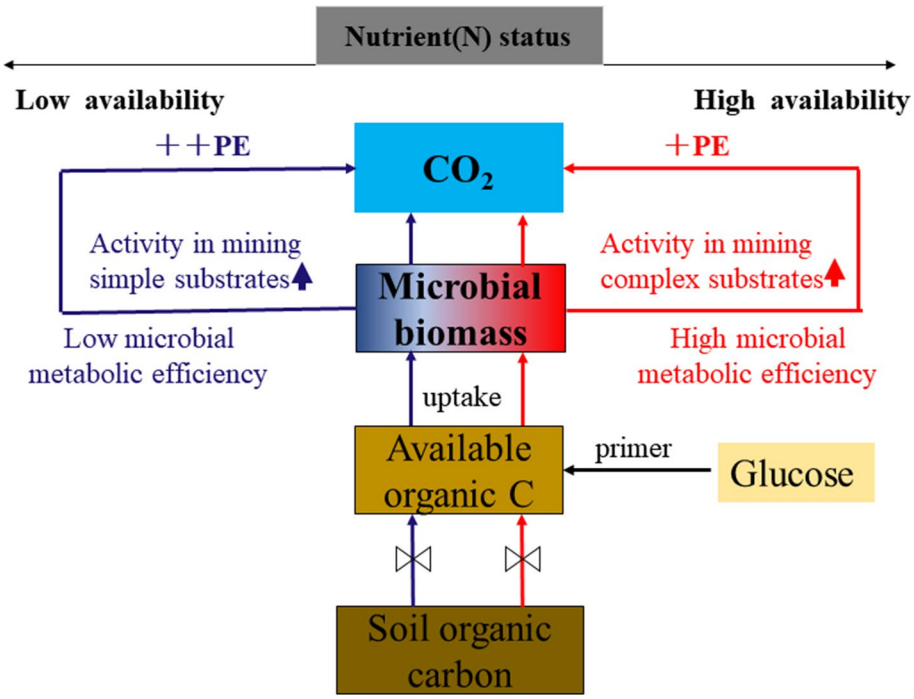

Fig. 7 The concept showing the labile C addition regulating the PE by altering microbial metabolic efficiency. Blue line indicates altered microbial relative substrate efficiency under lower N availability; the red line indicates the same under higher N availability

References

Blagodatskaya E, Kuzyakov Y (2008) Mechanisms of real and apparent priming effects and their dependence on soil microbial biomass and community structure: critical review. Biol Fertil Soils 45:115–131

Blagodatskaya EV, Blagodatsky SA, Anderson TH, Kuzyakov Y (2007) Priming effects in Chernozem induced by glucose and N in relation to microbial growth strategies. Appl Soil Ecol 37:95–105

Blagodatsky S, Blagodatskaya E, Yuyukina T, Kuzyakov Y (2010) Model of apparent and real priming effects: linking microbial activity with soil organic matter decomposition. Soil Biol Biochem 42:1275–1283

Bölscher T, Wadsö L, Börjesson G, Herrmann AM (2016) Differences in substrate use efficiency: impacts of microbial community composition, land use management, and substrate complexity. Biol Fertil Soils 52:547–559

Chen LY, Liu L, Mao C, Qin SQ, Wang J, Liu FT, Blagodatsky S, Yang GB, Zhang QW, Zhang DY, Yu JC, Yang YH (2018) Nitrogen availability regulates topsoil carbon dynamics after permafrost thaw by altering microbial metabolic efficiency. Nat Commun 9:3951

Chen RR, Senbayram M, Blagodatsky S, Myachina O, Dittert K, Lin XG, Blagodatskaya E, Kuzyakov Y (2014) Soil C and N availability determine the priming effect: microbial N mining and stoichiometric decomposition theories. Glob Chang Biol 20:2356–2367

Craine JM, Morrow C, Fierer N (2007) Microbial nitrogen limitation increases decomposition. Ecology 88:2105–2113

Currey PM, Johnson D, Sheppard LJ, Leith ID, Toberman H, van der Wal R, Dawson LA, Artz RRE (2010) Turnover of labile and recalcitrant soil carbon differ in response to nitrate and ammonium deposition in an ombrotrophic peatland. Glob Chang Biol 16:2307–2321

Derrien D, Plain C, Courty PE, Gelhaye L, Moerdijk-Poortvliet TCW, Thomas F, Versini A, Zeller B, Koutika LS, Boschker HTS (2014) Does the addition of labile substrate destabilise old soil organic matter? Soil Biol Biochem 76:149–160

Fang YY, Nazaries L, Singh BK, Singh BP (2018) Microbial mechanisms of carbon priming effects revealed during the interaction of crop residue and nutrient inputs in contrasting soils. Glob Chang Biol 24:2775–2790

Fierer N, Allen AS, Schimel JP, Holden PA (2003) Controls on microbial CO_2 production: a comparison of surface and subsurface soil horizons. Glob Chang Biol 9:1322–1332

Garcia-Pausas J, Paterson E (2011) Microbial community abundance and structure are determinants of soil organic matter mineralisation in the presence of labile carbon. Soil Biol Biochem 43:1705–1713

de Graaff MA, van Groenigen KJ, Six J, Hungate B, van Kessel C (2006) Interactions between plant growth and soil nutrient cycling under elevated CO_2: a meta-analysis. Glob Chang Biol 12:2077–2091

Hessen DO, Ågren GI, Anderson TR, Elser JJ, de Ruiter PC (2004) Carbon sequestration in ecosystems: the role of stoichiometry. Ecology 85:1179–1192

Hicks LC, Meir P, Nottingham AT, Reay DS, Stott AW, Salinas N, Whitaker J (2019) Carbon and nitrogen inputs differentially affect priming of soil organic matter in tropical lowland and montane soils. Soil Biol Biochem 129:212–222

Janssens IA, Dieleman W, Luyssaert S, Subke JA, Reichstein M, Ceulemans R, Ciais P, Dolman AJ, Grace J, Matteucci G, Papale D, Piao SL, Schulze ED, Tang J, Law BE (2010) Reduction of forest soil respiration in response to nitrogen deposition. Nat Geosci 3:315–322

Jiang X, Haddix ML, Cotrufo MF (2016) Interactions between biochar and soil organic carbon decomposition: effects of nitrogen and low molecular weight carbon compound addition. Soil Biol Biochem 100:92–101

Kuzyakov Y, Friedel J, Stahr K (2000) Review of mechanisms and quantification of priming effects. Soil Biol Biochem 32:1485–1498

Liljeroth E, Kuikman P, Van Veen J (1994) Carbon translocation to the rhizosphere of maize and wheat and influence on the turnover of native soil organic matter at different soil nitrogen levels. Plant Soil 161:233–240

Liu XJA, Finley BK, Mau RL, Schwartz E, Dijkstra P, Bowker MA, Hungate BA (2020) The soil priming effect: consistent across ecosystems, elusive mechanisms. Soil Biol Biochem 140:107617

Liu WX, Qiao CL, Yang S, Bai WM, Liu LL (2018) Microbial carbon use efficiency and priming effect regulate soil carbon storage under nitrogen deposition by slowing soil organic matter decomposition. Geoderma 332:37–44

Manzoni S, Taylor P, Richter A, Porporato A, Ågren GI (2012) Environmental and stoichiometric controls on microbial carbon-use efficiency in soils. New Phytol 196:79–91

Melillo JM, Aber JD, Muratore JF (1982) Nitrogen and lignin control of hardwood leaf litter decomposition dynamics. Ecology 63:621–626

Midwood AJ, Gebbing T, Wendler R, Sommerkorn M, Hunt JE, Millard P (2006) Collection and storage of CO_2 for ^{13}C analysis: an application to separate soil CO_2 efflux into root- and soil-derived components. Rapid Commun Mass Spectrom 20:3379–3384

Moorhead DL, Sinsabaugh RL (2006) A theoretical model of litter decay and microbial interaction. Ecol Monogr 76:151–174

Mooshammer M, Wanek W, Hämmerle I, Fuchslueger L, Hofhansl F, Knoltsch A, Schnecker J, Takriti M, Watzka M, Wild B, Keiblinger KM, Zechmeister-Boltenstern S, Richter A (2014) Adjustment of microbial nitrogen use efficiency to carbon:nitrogen imbalances regulates soil nitrogen cycling. Nat Commun 5:3694

Morrissey EM, Mau RL, Schwartz E, McHugh TA, Dijkstra P, Koch BJ, Marks JC, Hungate BA (2017) Bacterial carbon use plasticity, phylogenetic diversity and the priming of soil organic matter. ISME J 11:1890–1899

Naisse C, Girardin C, Davasse B, Chabbi A, Rumpel C (2015) Effect of biochar addition on C mineralisation and soil organic matter priming in two subsoil horizons. J Soils Sediments 15:825–832

Pinzari F, Maggi O, Lunghini D, Di Lonardo DP, Persiani AM (2017) A simple method for measuring fungal metabolic quotient and comparing carbon use efficiency of different isolates: application to Mediterranean leaf litter fungi. Plant Biosyst 151:371–376

Rumpel C, Kögel-Knabner I (2011) Deep soil organic matter—a key but poorly understood component of terrestrial C cycle. Plant Soil 338:143–158

Saiya-Cork KR, Sinsabaugh RL, Zak DR (2002) The effects of long term nitrogen deposition on extracellular enzyme activity in an Acer saccharum forest soil. Soil Biol Biochem 34:1309–1315

Sinsabaugh RL, Turner BL, Talbot JM, Waring BG, Powers JS, Kuske CR, Moorhead DL, Shah JJF (2016) Stoichiometry of microbial carbon use efficiency in soils. Ecol Monogr 86:172–189

Tian QX, Yang XL, Wang XG, Liao C, Li QX, Wang M, Wu Y, Liu F (2016) Microbial community mediated response of organic carbon mineralization to labile carbon and nitrogen addition in topsoil and subsoil. Biogeochemistry 128:125–139

Wang QK, Wang YP, Wang SL, He TX, Liu L (2014a) Fresh carbon and nitrogen inputs alter organic carbon mineralization and microbial community in forest deep soil layers. Soil Biol Biochem 72:145

Wang QG, Xu YZ, Lu ZJ, Bao DC, Guo YL, Lu JM, Zhang KH, Liu HB, Meng HJ, Qiao XJ, Huang HD, Jiang MX (2014b) Disentangling the effects of topography and space on the distributions of dominant species in a subtropical forest. Chin Sci Bull 59:5113–5122

Zhang ZY, Wang WF, Qi JX, Zhang HY, Tao F, Zhang RD (2019) Priming effects of soil organic matter decomposition with addition of different carbon substrates. J Soils Sediments 19:1171–1178

Zhang YL, Yao SH, Mao JD, Olk DC, Cao XY, Zhang B (2015) Chemical composition of organic matter in a deep soil changed with a positive priming effect due to glucose addition as investigated by ^{13}C NMR spectroscopy. Soil Biol Biochem 85:137–144